새로운 요소분해방법에 의한 쉘 유한요소의 개발

FORMULATION OF SHELL FINITE ELEMENTS BASED ON A NEW METHOD OF ELEMENT DECOMPOSITION

李 宰 泳*
Lee, Jae Young

요 약

이 연구에서는 새로운 쉘要素分解의 方法을 定立하고, 이에 의거하여 간단하고, 효율성이 높고, 普遍性이 큰 쉘 有限要素를 개발하고자 하였다. 實際의 要素는 概念的인 Translational Element와 Difference Element로 分解되며, 要素의 變位函數는 이 두 成分要素의 變位函數를 결합하여 얻는다. 要素分解의 基本假定을 달리함에 따라서 세가지의 基本形要素에 도달할 수 있다.

基本形要素를 보완하여 Locking現像을 제거하고 수렴성을 높히는 방안으로서 減着積分, 內部自有度의 追加 및 Mixed Fomulation을 검토하였으며, 要素의 Spurious Mode를 制御하는 방법을 고안하였다. 數値分析을 통해서 要素의 有效性과 効率性을 검정하였다.

ABSTRACT

A new method of element decomposition is suggested for simple, efficient, and generalized formulation of shell finite elements. The kernel of the method is to decompose conceptually the actual element into a translational element and a difference element. The actual element is obtained by combining the two component elements. The derived element can be classified into three basic types depending on how the element is decomposed.

A few complementary measures, to remove locking phenomena and thus improve the performance of the elements, have been studied. They are reduced integration, addition of internal degrees of freedom, and mixed formulation. A rational method of controlling spurious zero energy modes has also been devised. Validity and efficiency of the element with or without complementary measures have been examined through a series of numerical studies.

* 정회원, 전북대학교 농공학과 조교수, 공박
이 研究는 1986年度 韓國科學財團의 研究費 支援으로 遂行되었음.

이 논문에 대한 토론을 1988년 12월 31일까지 본학회에 보내주시면, 그 결과를 1989년 6월호에 게재하겠읍니다.

1. INTRODUCTION

There have been enormous efforts to find a good element, accurate, simple and generalized for shell analysis. As a result, a great number of shell elements have been developed, and more continue to be proposed. However, no one particular element has emerged as uniquely the best element. An element good for a certain type of problems may be poor for others. This study is another effort to find shell elements good for broad range of shell problems. The main theme of the study is the formulation of shell finite elements based on a new method of element decomposition.

Concept of element decomposition is not new and has been involved in many other plate and shell elements (Bazeley et al., 1965, Stolasky et al., 1984). In the present study, however, the method of decomposition is far more generalized with respect to element shape, number of nodes per element, number of d.o.f. per node, and most importantly the assumption on transverse shear strains.

2. NEW METHOD OF ELEMENT DECOMPOSITION

The actual element is termed the total element, and is decomposed into a translational element and a difference element. The translational element is defined completely by the nodal translations, and the difference element represents the difference between the actual element and the translational element. The nodal displacements are decomposed into the part for the translational element and the remaining one for the difference element. The displacements within each element are determined by independent interpolation of the respective part of the nodal displacements. The total element is built by superposition of the two component elements. The decomposition is intended not only to simplify and systematize the formulation but also to ensure the rigid body displacements. One can arrive at different types of elements depending on how the nodal displacements are decomposed.

Most of the existing shell elements have five or six d.o.f. per node. The present method is valid for both cases. In this paper, however, discussion is limited to the formulation based on five d.o.f. which is far more common. Its extension to six d.o.f. formulation is to be presented in a forthcoming paper.

2.1. Total element

The total element represents the actual displacement field, and for five d.o.f. case, is defined by,

$$\Delta = \lfloor u \; v \; w \; \alpha \; \beta \rfloor = \lfloor \delta \; \theta \rfloor \tag{1}$$

in which $\delta = \lfloor u \; v \; w \rfloor$ denotes a vector with translation components expressed in x, y, and z Cartesian coordinate system, and $\theta = \lfloor \alpha \; \beta \rfloor$ a vector with rotations about local x and y axes defined on the tangent plane.

The nodal displacement of the total element should be equivalent to the actual nodal displacements. The element nodal d.o.f are denoted by Δ^e

$$\Delta^e = \lfloor \Delta_1 \cdots \Delta_n \rfloor = \lfloor \delta_1 \; \theta_1 \cdots \delta_n \; \theta_n \rfloor \tag{2}$$

in which n is the number of nodes in each element.

2.2. Translational element

The translational element is defined completely by nodal translations. The element is denoted with superscript t.

$$\Delta^t = \lfloor \delta^t \; \theta^t \rfloor \tag{3}$$

The translations represented by the translational elemnt should match the actual nodal translations at each node,

$$\delta_i^t = \delta_i,$$
$$\Delta^{te} = \lfloor \delta_1^t \; \theta_1^t \cdots \delta_n^t \; \theta_n^t \rfloor = \lfloor \delta_1 \theta_1^t \cdots \delta_n \theta_n^t \rfloor \tag{4}$$

2.3. Difference element

The difference element represents the difference between the total element and the translational element. The element is denoted with superscript d.

$$\Delta^d = \Delta - \Delta^t \tag{5}$$

The nodal translations of the element are always zero,

$$\delta_i^d = 0, \quad \text{for } i = 1, \cdots, n \tag{6}$$

Therefore,

$$\Delta^{de} = [\, \delta_1^d \theta_1^d \cdots \delta_n^d \theta_n^d \,] = [\, 0\ \theta_1^d \cdots 0\ \theta_n^d \,] \tag{7}$$

3. REPRESENTATION OF DISPLACEMENET FIELD

The nodal d.o.f. can be decomposed in many different ways. One may logically think of four possibilities depending on whether any or all of the component elements are subject to the Kirchhoff assumption. One possibility, in which the difference element satisfies the Kirchhoff assumption and the translational element does not, is excluded in the present study because it may not allow rigid body displacement. The other three types of decomposition are designated as type I, type II and type III decompositions. Interpolations of the displacement field from the nodal displacements are expressed by the displacement function matrix **T** which has the same format for all types of element decomposition.

3.1. Type I decomposition

The displacement fields are decomposed so that both the translational and the difference elements can satisfy the Kirchhoff assumption. First the nodal rotations of the translational element are evaluated as a function of surface normal displacement. And then, the nodal rotations of the difference element are obtained by $\theta^d = \theta - \theta^t$. The translations within the translational element are interpolated from nodal translations, and the intra-element normal displacement of the difference element is determined by nodal values of θ^d.

3.1.1. Translational element

The nodal displacements of the translational element are given by Eqn.(4). The translations are obtained by interpolation of nodal values.

$$\delta^t = \sum_{i=1}^{n} N_i \delta_i \quad \text{or} \quad \delta^t = \sum_{i=1}^{n} N_i \delta_i = \sum_{i=1}^{n} N_i \mathbf{R} \delta_i \tag{8}$$

in which N_i is the shape function for node i, and R denotes the (3×3) rotation matrix evaluated at point under consideration. Displacements expressed in local coordinates are denoted in italics, such as u, v, w, and δ. One can relate δ^t to the element nodal d.o.f. in the form of

$$\delta^t = \mathbf{L}\, \Delta^e \tag{9}$$

in which

$$\underset{3\times 5n}{\mathbf{L}^T} = [\, \mathbf{L}_1 \mathbf{L}_2 \mathbf{L}_3 \,] \tag{10}$$

$$\underset{1\times 5n}{\mathbf{L}_k} = [\, \underset{1\times 3}{\mathbf{H}_{k1}}\ \underset{1\times 2}{\mathbf{0}}\ \mathbf{H}_{k2}\, 0 \cdots \mathbf{H}_{kn}\, 0 \,] \text{ for } k = 1, 2, 3 \tag{11}$$

$$\text{with } \mathbf{H}_{ki} = N_i [\, \mathbf{R}_{k1}\ \mathbf{R}_{k2}\ \mathbf{R}_{k3} \,] \tag{12}$$

Since the translational element, in type I decomposition, is subject to the Kirchhoff assumption, the rotation can be expressed in terms of the surface normal translation.

$$\theta^t = \begin{Bmatrix} \alpha^t \\ \beta^t \end{Bmatrix} = \begin{Bmatrix} w^t{}_{,x} \\ w^t{}_{,y} \end{Bmatrix} = \begin{bmatrix} \mathbf{L}_{3,x} \\ \mathbf{L}_{3,y} \end{bmatrix} \Delta^e \tag{13}$$

The row vectors $L_{3,x}$ and $L_{3,y}$ are obtained from

$$\begin{bmatrix} \mathbf{L}_{3,x} \\ \mathbf{L}_{3,y} \end{bmatrix} = [\, \mathbf{H}'_{31}\ \ 0\ \ \underline{\mathbf{H}}'_{32}\ \ 0 \cdots \underline{\mathbf{H}}'_{3n}\ \ 0 \,]$$
$$= \mathbf{J}^{-1} [\, \underline{\mathbf{H}}'_{31}\ 0\ \underline{\mathbf{H}}'_{32}\ 0 \cdots \underline{\mathbf{H}}'_{3n}\ 0 \,] \tag{14}$$

in which **J** denotes the Jacobian matrix, and

$$\mathbf{H}'_{3k} = \begin{bmatrix} \mathbf{H}_{3k,x} \\ \mathbf{H}_{3k,y} \end{bmatrix} \quad \text{and} \quad \underline{\mathbf{H}}'_{3k} = \begin{bmatrix} \mathbf{H}_{3k,\xi} \\ \mathbf{H}_{3k,\eta} \end{bmatrix} \tag{15}$$

The natural coordinates ξ, η are either the two independent area coordinates for a triangular element or the $(-1, +1)$ range intrinsic coordinates for a quadrilateral element. Now, the displacements of the translational element can be written in terms of the element nodal d.o.f. of the total element.

$$\Delta^t = \begin{Bmatrix} u^t \\ v^t \\ w^t \\ \alpha^t \\ \beta^t \end{Bmatrix} = \begin{bmatrix} L_1 \\ L_2 \\ L_3 \\ L_{3,x} \\ L_{3,y} \end{bmatrix} \Delta^e \tag{16}$$

3.1.2. Difference element

Although the total element is not determined yet, the nodal contribution of the difference element can be obtained using the relation

$$\Delta^d = \Delta - \Delta^t \tag{17}$$

or in local coordinates,

$$\Delta^d = \Delta - \Delta^t \tag{18}$$

The nodal translations consists of the contribution of the translational element only.

Therefore,

$$\delta_i^t = \delta_i \quad \text{and} \quad \delta_i^d = 0 \tag{19}$$

The nodal rotations of difference element are derived directly from Eqns. (5) and (13),

$$\begin{aligned} \theta_i^d &= \theta_i - \theta_i^t \\ &= [-H'_{31(i)} \quad 0 \quad -H'_{32(i)} \quad 0 \quad \cdots -H'_{31(i)} \quad 1 \\ &\quad \cdots -H'_{3n(i)} \quad 0\,]\Delta^e \end{aligned} \tag{20}$$

in which $H'_{3k(i)}$ implies H'_{3k} evaluated at node i and I is a (2×2) unit matrix. If one denotes with underlines the rotations expressed in natural coordinates such as

$$\underline{\theta} = \begin{Bmatrix} \underline{\alpha} \\ \underline{\beta} \end{Bmatrix} \qquad \theta^d = \begin{Bmatrix} \alpha^d \\ \beta^d \end{Bmatrix} \tag{21}$$

then,

$$\theta^d = J\,\theta^d \quad \text{or} \quad \theta^d = J^{-1}\,\theta^d \tag{22}$$

Therefore, from Eqns. (20) and (22)

$$\begin{aligned} \theta_i^d &= J_{(i)}\,\theta_i^d \\ &= [-H'_{31(i)}\,0 \cdots -H'_{31(i)}\,J_{(i)} \cdots -H'_{3n(i)}\,0\,]\Delta^e \end{aligned} \tag{23}$$

where $J_{(i)}$ is the Jacobian matrix evaluated at node i. Now, the nodal rotations of the difference element with respect to natural coordinates can be expressed in terms of the element nodal d.o.f.

$$\theta^{de} = Q\,\Delta^e \tag{24}$$

$$\underline{\theta}^{de} = \begin{Bmatrix} \underline{\theta}^d{}_{(1)} \\ \underline{\theta}^d{}_{(2)} \\ \cdot \\ \cdot \\ \cdot \\ \underline{\theta}^d{}_{(n)} \end{Bmatrix} \text{ and}$$

$$Q = \begin{bmatrix} -H'_{31(1)} & J_{(1)} & -H'_{32(1)} & 0 \cdots & -H'_{3n(1)} & 0 \\ -H'_{31(2)} & 0 & -H'_{32(2)} & J_{(2)} \cdots & -H'_{3n(2)} & 0 \\ \cdot & \cdot & \cdot & \cdot \cdots & \cdot & \cdot \\ \cdot & \cdot & \cdot & \cdot \cdots & \cdot & \cdot \\ \cdot & \cdot & \cdot & \cdot \cdots & \cdot & \cdot \\ -H'_{31(n)} & 0 & -H'_{32(n)} & \cdot \cdots & -H'_{3n(n)} & J_{(n)} \end{bmatrix} \tag{25}$$

There exists a functional relationship, equivalent to Eqn.(13), between the surface normal displacements and the rotations of the difference element.

$$\begin{Bmatrix} \alpha^d \\ \beta^d \end{Bmatrix} = \begin{Bmatrix} w^d_{,x} \\ w^t_{,y} \end{Bmatrix} \tag{26}$$

Now, the difference element will be constructed such that θ^d at each node satisfies the nodal value given by Eqn. (24). The surface normal translation w^d can be defined in terms of generalized coordinates.

$$w^d = \underset{1\times3n}{p}\ \underset{3n\times1}{a} \tag{27}$$

with

$$\mathbf{p}=\lfloor 1\ \xi\ \eta\ \cdots\xi^{p}\eta^{q}\rfloor \text{ and } \mathbf{a}^{T}=\lfloor a_1\ a_2\ \cdots a_{3n}\rfloor \quad (28)$$

in which $\mathbf{p}$ is a vector of polynomial terms selected from Pascal's triangle and $\mathbf{a}$ is a vector of generalized coordinates.

$$\underset{3n\times 1}{\underline{\Theta}^{de}}=\underset{3n\times 3n}{\mathbf{A}}\ \underset{3n\times 1}{\mathbf{a}} \quad (29)$$

with

$$\Theta^{de}=\begin{Bmatrix}0\\ \underline{\alpha}_1^{d}\\ \underline{\beta}_1^{d}\\ \cdot\\ \cdot\\ \cdot\\ 0\\ \underline{\alpha}_n^{d}\\ \underline{\beta}_n^{d}\end{Bmatrix} \text{ and } \mathbf{A}=\begin{bmatrix}\mathbf{p}_1\\ \mathbf{p},\xi_1\\ \mathbf{p},\eta_1\\ \cdot\\ \cdot\\ \cdot\\ \mathbf{p}_n\\ \mathbf{p},\xi_n\\ \mathbf{p},\eta_n\end{bmatrix} \quad (30)$$

in which $\mathbf{p}_{(i)}$, $\mathbf{p},_{\xi(i)}$ and $\mathbf{p},_{\eta(i)}$ represent respectively $\mathbf{p}$, $\mathbf{p},_{\xi}$ and $\mathbf{p}_{\eta}$ evaluated at node i. Therefore,

$$\mathbf{a}=\mathbf{A}^{-1}\ \underline{\Theta}^{de}=\mathbf{G}\ \underline{\theta}^{de} \quad (31)$$

in which $\mathbf{G}$ is a $(3n\times 2n)$ matrix obtained from $\mathbf{A}^{-1}$ by removing the columns corresponding to zero entries in vector Θ^{de}. Subsitution of Eqn. (31) in (27) yields

$$w^{d}=\mathbf{p}\ \mathbf{G}\ \underline{\theta}^{de}=\mathbf{p}\ \mathbf{G}\ \mathbf{Q}\ \Delta^{e} \quad (32)$$

Since only p in the above equation is a function of coordinates,

$$\theta^{d}=\begin{Bmatrix}\alpha^{d}\\ \beta^{d}\end{Bmatrix}=\begin{Bmatrix}w^{d}_{,x}\\ w^{d}_{,y}\end{Bmatrix}=\begin{bmatrix}\mathbf{p}_x\\ \mathbf{p}_y\end{bmatrix}\mathbf{G}\ \mathbf{Q}\ \Delta^{e} \quad (33)$$

The displacement field of the difference element is constructed by combining Eqns. (19), (32) and (33).

$$\Delta^{d}=\begin{Bmatrix}u^{d}\\ v^{d}\\ w^{d}\\ \alpha^{d}\\ \beta^{d}\end{Bmatrix}=\begin{bmatrix}0\\ 0\\ \mathbf{p}\ \mathbf{G}\ \mathbf{Q}\\ \mathbf{p},_x\ \mathbf{G}\ \mathbf{Q}\\ \mathbf{p},_y\ \mathbf{G}\ \mathbf{Q}\end{bmatrix}\Delta^{e} \quad (34)$$

3.1.3. Total element

The displacement function matrix for the total element is obtained by addition of Eqns. (16) and (34).

$$\Delta=\Delta^{t}+\Delta^{d}=\begin{bmatrix}\mathbf{L}_1\\ \mathbf{L}_2\\ \mathbf{L}_3+\mathbf{p}\ \mathbf{G}\ \mathbf{Q}\\ \mathbf{L}_{3,x}+\mathbf{p},_x\ \mathbf{G}\ \mathbf{Q}\\ \mathbf{L}_{3,y}+\mathbf{p},_y\mathbf{G}\ \mathbf{Q}\end{bmatrix}\Delta^{e}=\mathbf{T}\ \Delta^{e} \quad (35)$$

with the displacement function matrix,

$$\underset{5\times 5n}{\mathbf{T}}=\begin{bmatrix}\mathbf{T}_1\\ \cdot\\ \cdot\\ \cdot\\ \mathbf{T}_5\end{bmatrix}=\begin{bmatrix}\mathbf{L}_1\\ \cdot\\ \cdot\\ \cdot\\ \mathbf{L}_{3,y}+\mathbf{p},_y\mathbf{G}\ \mathbf{Q}\end{bmatrix} \quad (36)$$

3.2. Type II decomposition

In type II decomposition, the translational element satisfies the Kirchhoff assumption, and therefore, is identical to that of type I decomposition. The translations of the difference element are restrained, i.e., $\delta^{d}=0$, while transverse shear deformations are included. The rotations are evaluated by independent interpolation of the nodal values of α^{d}_{i} and β^{d}_{i}, or θ^{d}_{i}. The displacement function matrix is presented below without derivation due to limited space. Its detailed derivation is given elsewhere (Lee, 1986).

$$\begin{bmatrix}\mathbf{T}_1\\ \mathbf{T}_2\\ \mathbf{T}_3\end{bmatrix}=\begin{bmatrix}\mathbf{L}_1\\ \mathbf{L}_2\\ \mathbf{L}_3\end{bmatrix}$$
$$\begin{bmatrix}\mathbf{T}_4\\ \mathbf{T}_5\end{bmatrix}=\begin{bmatrix}\mathbf{L}_{3,y}\\ \mathbf{L}_{3,y}\end{bmatrix}+\mathbf{J}^{-1}\mathbf{N}\ \mathbf{Q} \quad (37)$$

with

$$\underset{2\times 2n}{\mathbf{N}} = \begin{bmatrix} N_1 & 0 & N_2 & 0 \cdots N_n & 0 \\ 0 & N_1 & 0 & N_2 \cdots 0 & N_n \end{bmatrix} \tag{38}$$

3.3. Type Ⅲ decomposition

In type Ⅲ decomposition, the rotation of the translational element and the translations of the difference element are restrained. The translations of the translational element and the rotations of the difference element are obtained by independent interpolation of corresponding nodal values. Thus, the translations of the translational element are retained as in the type Ⅰ and Ⅱ decompositions, while all the translations of the difference element are suppressed, i.e., $\delta^d=0$. The rotations of the difference element are equivalent to that of the total element.

The type Ⅲ decomposition leads to an element similar to wellknown Ahmad's degenerated shell element (Ahmad et al., 1970). In Ahmad's element, the nodal rotations are first converted into translations in global coordinates and then these translations are interpolated to desired points, e.g., integration points. This type of interpolation, physically loyal to the degeneration concepts, prevents rigid body rotation of a curved element. That is the reason why the degenerated shell element performs poorly for the quarter cylinder test case subject to pure bending (Lee, 1986). It is obvious that the interpolation of θ^d allows rigid body rotations, as does isoparametric interpolation of translational d.o.f. (Cook, 1981). Interpolation of θ^d rather than θ^d is to maintain geometric isotropy. The implementation of the type Ⅲ element as well as its formulation is simpler than that of the degenerated shell element. The displacement matrix is given below.

$$\begin{bmatrix} \mathbf{T}_1 \\ \mathbf{T}_2 \\ \mathbf{T}_3 \end{bmatrix} = \begin{bmatrix} \mathbf{L}_1 \\ \mathbf{L}_2 \\ \mathbf{L}_3 \end{bmatrix} \qquad \begin{bmatrix} \mathbf{T}_4 \\ \mathbf{T}_5 \end{bmatrix} = \mathbf{J}^{-1}\,\mathbf{N}\,\mathbf{Q}_0 \tag{39}$$

with

$$\underset{2n\times 5n}{\mathbf{Q}_0} = \begin{vmatrix} 0 & \underset{2\times 3}{\mathbf{J}_{(1)}} & 0 & 0 & \cdots & 0 & 0 \\ \underset{2\times 3}{0} & \underset{2\times 3}{0} & \underset{2\times 3}{0} & \underset{2\times 3}{\mathbf{J}_{(2)}} & \cdots & 0 & 0 \\ \cdot & \cdot & \cdot & \cdot & \cdots & \cdot & \cdot \\ 0 & 0 & 0 & 0 & \cdots & 0 & \mathbf{J}_{(n)} \end{vmatrix} \tag{40}$$

4. STRAIN-DISPLACEMENT RELATIONSHIP

The displacement field within an element has been related to the nodal displacements by displacement function matrix. Differentiation of the matrix yields the strain-nodal displacement relationship which is directly involved in the stiffness matrix evaluation.

In a situation where the transverse shear strains are zero or constant through the thickness, the displacement field can be represented in terms of the midsurface translations and rotations.

$$\begin{Bmatrix} u' \\ v' \\ w' \end{Bmatrix} = \begin{Bmatrix} u \\ v \\ w \end{Bmatrix} - \frac{1}{2} t\zeta \begin{bmatrix} 1 & 0 \\ 0 & 1 \\ 0 & 0 \end{bmatrix} \begin{Bmatrix} \alpha \\ \beta \end{Bmatrix}$$

$$= \left[\begin{bmatrix} \mathbf{T}_1 \\ \mathbf{T}_2 \\ \mathbf{T}_3 \end{bmatrix} - \frac{1}{2} t\zeta \begin{bmatrix} \mathbf{T}_4 \\ \mathbf{T}_5 \\ 0 \end{bmatrix} \right] \Delta^e \tag{41}$$

where $[u'v'w']$ represents the translations of a point on the surface a distance $\frac{1}{2}(t\zeta)$ away from the midsurface, whereas $[u\ v\ w]$ are the translations on the midsurface. Thus, one can establish a general form of the strain-nodal displacement relationship as follows:

$$\varepsilon = \begin{Bmatrix} \varepsilon_x \\ \varepsilon_y \\ \gamma_{xy} \\ \gamma_{yz} \\ \gamma_{xz} \end{Bmatrix} = \begin{bmatrix} \mathbf{B}^m - 1/2\, t\zeta\, \mathbf{B}^b \\ \mathbf{B}^s \end{bmatrix} \Delta^e = \mathbf{B}\,\Delta^e \tag{42}$$

in which the strain components are defined in local coordinates, and

$$\underset{3\times5n}{\mathbf{B}^m}=\begin{bmatrix} T_{1,x} \\ T_{2,y} \\ T_{1,y}+T_{2,x} \end{bmatrix},\quad \underset{3\times5n}{\mathbf{B}^b}=\begin{bmatrix} T_{4,x} \\ T_{5,y} \\ T_{4,y}+T_{5,x} \end{bmatrix}$$

$$\text{and } \underset{2\times5n}{\mathbf{B}^s}=\begin{bmatrix} T_{3,x} \\ T_{3,y} \end{bmatrix}-\begin{bmatrix} T_4 \\ T_5 \end{bmatrix} \tag{43}$$

5. ELEMENT STIFFNESS MATRIX

Once the strain-displacement relationship is established, the stiffness matrix can be evaluated directly using following standard equation of displacement finite element formulation:

$$\mathbf{k}^e=\int_v \mathbf{B}^T\mathbf{D}\,\mathbf{B}\,dV \tag{44}$$

in which $\mathbf{k}^e$ is the element stiffness matrix, and $\mathbf{D}$, the (5×5) stress-strain matrix. In association with Eqn.(42), the matrix $\mathbf{D}$ is partitioned as

$$\underset{5\times5}{\mathbf{D}}=\begin{vmatrix} \underset{3\times3}{\mathbf{D}^p} & \underset{3\times2}{\mathbf{D}^{ps}} \\ \underset{2\times3}{\mathbf{D}^{sp}} & \underset{2\times2}{\mathbf{D}^s} \end{vmatrix} \tag{45}$$

in which $\mathbf{D}^p$ and $\mathbf{D}^s$ are symmetric, and $\mathbf{D}^{sp}=(\mathbf{D}^{ps})^T$. Substituting Eqns. (43) and (45) into Eqn. (44), one obtains

$$\mathbf{k}^e=\int_v\begin{bmatrix} \mathbf{B}^m-1/2\,t\,\zeta\mathbf{B}^b \\ \mathbf{B}^s \end{bmatrix}^T\begin{bmatrix} \mathbf{D}^p & \mathbf{D}^{ps} \\ \mathbf{D}^{sp} & \mathbf{D}^s \end{bmatrix}\times\begin{bmatrix} \mathbf{B}^m-1/2\,t\,\zeta\mathbf{B}^b \\ \mathbf{B}^s \end{bmatrix}dV \tag{46}$$

The integration in the thickness direction can be performed explicitly. And integration of $\xi\,d\xi$ yields zero. For isotropic or stratified anisotropic matrials, $\mathbf{D}^{ps}=0$, and the stiffness matrix equation can be simplified further.

$$\mathbf{k}^e=t\int_A(\mathbf{B}^{mT}\mathbf{D}^p\mathbf{B}^m+\tfrac{1}{12}t^2\mathbf{B}^{bT}\mathbf{D}^p\mathbf{B}^b+\mathbf{B}^{sT}\mathbf{D}^s\mathbf{B}^s)\times|\mathbf{J}|\,dA \tag{47}$$

If the material is isotropic,

$$\mathbf{D}^p=\frac{E}{(1-\nu^2)}\begin{bmatrix} 1 & \nu & 0 \\ \nu & 1 & 0 \\ 0 & 0 & (1-\nu)/2 \end{bmatrix}$$

$$\mathbf{D}^s=\frac{E}{2k(1+\nu)}\begin{bmatrix} 1 & 0 \\ 0 & 1 \end{bmatrix} \tag{48}$$

in which E is the Young's modulus, and ν is the Poisson's ratio. The constant k is a factor to compensate the strain energy for transverse shear displacement approximation.

6. IMPROVEMENT OF THE FORMULATION

According to the numerical study (Fig.1-Fig. 4) presented in the next section, the greatest trouble with the newly formulated elements, similarly to the degenerated shell element, is the transverse shear locking. These elements, like many other shell elements with inclusion of transverse shear deformation, show unacceptably slow convergence under thin shell situation. A few complementary measures to alleviate the shear locking have been examined as described in this section.

6.1. Reduced integration

Reduced integration (with 2×2 rule) improves remarkably the convergence of the degenerated shell element of quadrilateral shape (Zienkiewicz et al., 1971). Similar results are obtained in the case of the type III element as well. However, distorsion of element shape diminishes the effectiveness of reduced integration, and thus, triangular or severely distorted elements cannot take advantage of reduced integration. Collapsed quadrilateral elements perform no better than triangular elements. For 6-node triangular elements, a 3-point integration, as opposed to 6-or 7-point rules, may be regarded as a reduced scheme.

6.2. Addition of nodeless d.o.f.

Tsach (1981) observed that an element does not lock when the interpolated shear strain function contains more variables than the number of equations obtained when equating the shear strains to zero. Therefore, one can avoid locking either by increasing the number of variables or by reducing the number

of equations. Reduced integration is equivalent to reducing the number of equations. One may increase the number of variables simply by adding nodeless d.o.f. Cook (1972) advocated the use of a bubble mode in eight-noded plate elements. Takemoto and Cook (1973) studied analogous treatment of the degenerated shell element. Choi (1986) proposed addition of nonconforming modes to the degenerate shell element of quadrilateral shape. Analogous nonconforming modes for triangular elements can easily be derived (Lee, 1988).

In this study, addition of bubble and nonconforming modes has been examined chiefly for triangular elements with or without reduced integration. These modes have been applied only to translational d.o.f. Fig.2 shows convergence test results for the pinched thin cylinder case, which is highly locking sensitive. Addition of nonconforming and bubble modes brings remarkable improvement when full order integration is applied. But equivalent improvement can be achieved by use of the a bubble mode alone together with reduced integration. This test case fails due to spurious modes when both nonconforming and bubble modes are simultaneously applied in combination with reduced integration.

6.3. Mixed formulation

Lee and Pian (1978) demonstrated the improvement of plate and shell elements by the mixed formulation based on the Hellinger-Reissner principle. A mixed model can be established by applying the principle to the type Ⅲ decomposition(Lee, 1988). The improvement by the mixed model is equivalent to that of reduced integration. Mixed model requires much more computational cost. But, this alternative formulation may be a good substitute for reduced integration if it should be avoided.

6.4. Control of zero-energy modes

According to the numerical tests with the type Ⅲ element, addition of a bubble mode in combination with reduced integration seems to be the most effective and efficient measure to relieve the shear locking. However, the element suffers from spurious modes for some cases with minimum boundary constraints, e.g., four-corner-supported square plate case. Such cases are not common in practical situation, but critical enough to invalidate the generality of the element. Therefore, spurious modes should be controlled even in such extreme cases.

In an attempt to remove spurious modes, Kavanagh and Key (1972) formed the element stiffness matix by the sum

$$\mathbf{K}=\alpha\mathbf{K}_{\text{full}}+(1-\alpha)\mathbf{K}_{\text{red}} \tag{49}$$

where $\mathbf{K}_{\text{full}}$ and $\mathbf{K}_{\text{red}}$ represent stiffness matrices respectively by full and reduced integration, and is better than selective reduced integration, because its precedure is simpler and it does not destroy geometric isotropy.

Cook(1972) and Takemoto and Cook (1973) suggested multiplying k_c by (1+e) prior to condensation of the nodeless d.o.f., where e is a small number and k_c represents the diagonal entries of $\mathbf{k}_{ee}$, the part associated with the nodeless d.o.f. in the uncondensed element stiffness matrix

$$\mathbf{k}'=\begin{bmatrix}\mathbf{k}_{rr} & \mathbf{k}_{re}\\ \mathbf{k}_{er} & \mathbf{k}_{ee}\end{bmatrix} \tag{50}$$

α has a value between zero and one. The scheme

Cook (1972) reported that the most suitable value of e is 0.003. That is not true, at least for the shell elements examined in this study (Lee, 1988). The dilemma in the above two schemes is that too small α or e value cannot control spurious modes sufficiently, while an excessive value induces locking. Unfortunately, the best α or e value depends on the thickness and the shape of the shell, and

cannot be determined uniquely.

This study suggests a more consistent method of controlling spurious modes. That is to apply full order integration to $\mathbf{k}_{ee}$ and reduce integration to the rest part of the uncondensed element stiffness matrix k'.

Application of the method slightly retards the convergence rate, but secures the control of spurious modes. The method does not rely on artificial numbers such as α or e, and therefore, does not restrict the generality of the element.

7. NUMERICAL STUDY

Effectiveness and validity of the present formulation have been examined through extensive numerical tests. The formulation is also viewed in comparison with the popular degenerated shell element. The effects and limitations of various complementray devices are numerically demonstrated.

7.1. Rigid body mode test

Existence of the rigid body modes can be discerned either by examining the deformation of the element under rigid body nodal displacements, or by examining the eigenvalues of the element stiffness matrix. Both methods are employed in the present study. The type I and II elements seem to satisfy the requirement for all cases, while reduced integration is required for the type III element to secure the 6 rigid body modes. On the other hand, the Ahmad's degenerated shell element even with reduced integration devoids rigid body modes, and cannot represent rigid body rotations when the curvature of the element is significantly large. The deficiency of the rigid body modes seems to be the main source of locking in this element.

7.2. Examination of zero energy modes

Rigid body modes are a kind of zero energy modes necessary for convergence. But there are zero energy modes of another kind. They are spurious modes which are unnecessary or harmful.

Distinction between spurious zero energy modes and rigid body modes can be made by close examination of eigenvectors associated with zero eigenvalues of the element stiffness matrix. This is usually achieved by graphical visualization of those eigenvectors, which shows that the type III element with a bubble mode suffers from spurious modes and that they can be properly controlled by remedies mentioned in the previous section.

Examination of the number of zero eignvalues suggests that each complementary device is accompanied by zero energy modes. Thus, addition of more complementary devices implies more spurious modes. Simultaneous application of bubble and nonconforming modes together with reduced integration induces too many zero energy modes to control. But, in general, the method of spurious mode control suggested in the present study turned out to be effective in suppressing the most of the spurious modes.

7.3. Geometric isotropy test

Geometric isotropy of an element can also be examined by the eigenvalues of the element stiffness matrix. An element is regarded as satisfying geometric isotropy, if the eigenvalues are not altered by rotation of the element. It has been found that the type I, II and III elements as well as the degenerated shell element retain the geometric isotropy, and that most of the complementary devices do not destroy the condition. However, this is not true for the following two complementary measures:

1) selective reduced integration

2) mixed formulation with different number of terms in the assumed normal strain and in the shear strains.

The geometric isotropy is violated by the above two methods. Therefore, they are undesirable, if not rejectable.

7.4. Patch tests

Patch test is commonly used to examine the constant strain state of an element which is the most important requirement for convergence to the correct solution(Cook, 1981, Zienkiewicz, 1977). The following four cases have been used in the patch tests in the present study.

case Ⅰ :cantilever plate subjected to uniform tensile load at the free end.

case Ⅱ :cantilever plate subjected to uniformly distributed moment at the free end.

case Ⅲ :fixed free quarter cylinder subjected to uniformly distributed moment at the free end.

case Ⅳ :sphere under uniform pressure.

The type Ⅰ, Ⅱ and Ⅲ elements pass the test for case Ⅰ and Ⅱ, and pass infinitesimally for case Ⅲ and Ⅳ. A curved shell element gives correct convergence as long as it passes the patch test at least in infinitesimal sense(Zienkiewicz, 1971). Therefore, the present formulation is considered to fulfill the patch test. On the other hand, the degenerated element fails the test for case Ⅲ. This may be the reason why this element shows poor convergence for curved shells with dominant bending actions(Lee, 1988).

7.5. Convergence tests

The convergence behavior of the newly develop elements and the degenerated shell element have been investigated using the following two test cases:

case Ⅰ :cylindrical shell roof test case.

case Ⅱ :thin pinched cylinder test case.

These two cases are widely uses as bench mark problems for shell elements. Detailed descriptions about the problems are given elsewhere(Cook, 1981), and avoided here due to space limitation.

The convergence pattern of the new elements and that of the conventional degenerated shell element are compared in Fig.1 and Fig.2. It should be noted that the degenerated shell element of quadrilateral shape gives convergence to the value approximately 7 % smaller than the correct solution for case Ⅱ, while the new elements show correct convergence. This locking phenomena of the degenerated shell element can be related to the fact that the element fails the patch test for the case of constant bending state and devoids rigid body modes when the element has significant curvature. Other numerical tests revealed that this tendency is conspicuous when the curvature of the structure is significant and the bending action is dorminant. This difficulty has been overcome by the new method of element decomposition which enables constant bending state and assures the required rigid body modes.

Covergence with various complementary devices are compared in Fig.3 and Fig.4. Reduced integration is quite effective for quardrilateral shaped elements, but not for triangular ones. Elements with triangular shape show noticeably slower convergence than quadrilateral elements. The convergence of triangular elements are almost unacceptably slow especially for case Ⅱ. Reduced integration alone is not sufficient for this case. Therefore, addition of bubble or nonconforming modes is essentially required for triangular element to secure satisfactory convergence speed.

8. CONCLUSIONS

A generalized and systematic procedure of shell element formulation has been established on the basis of new method of element decomposition. Three types of elements, designated as types

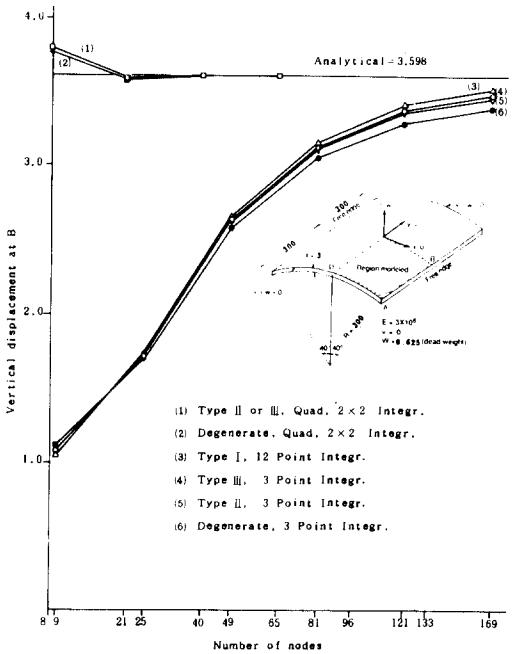

Fig.1. Comparison of the new elements with the degenerated shell element. (cylindrical shell roof test case)

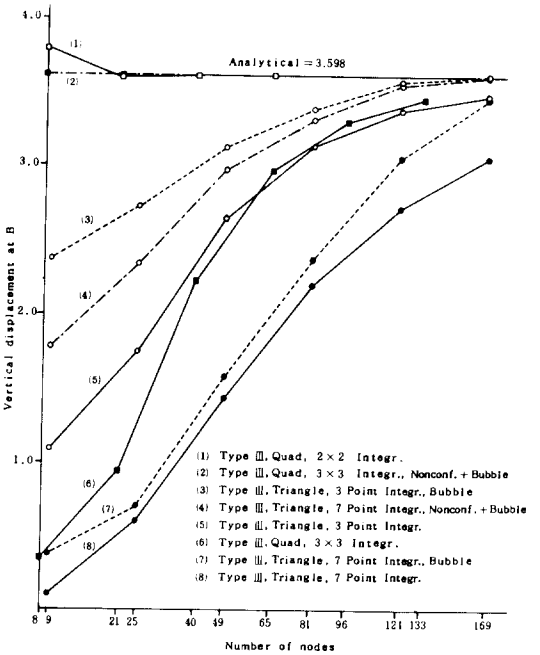

Fig.3. Effect of complementary measures. (cylindrical shell roof test case)

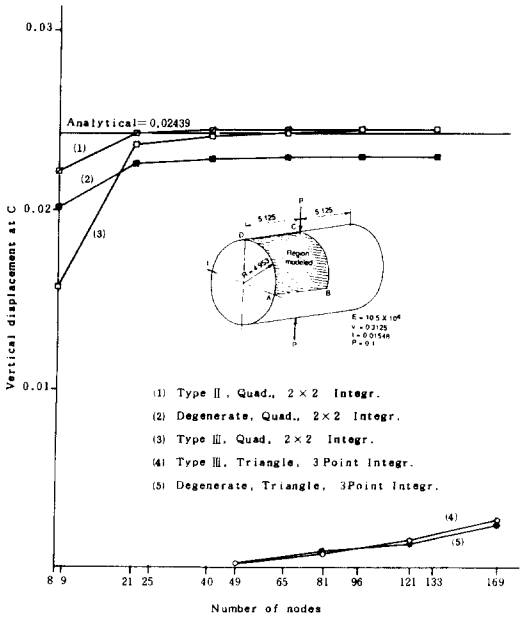

Fig.2. Comparison of the new elements with the degenerated shell element. (pinched thin cylinder test case)

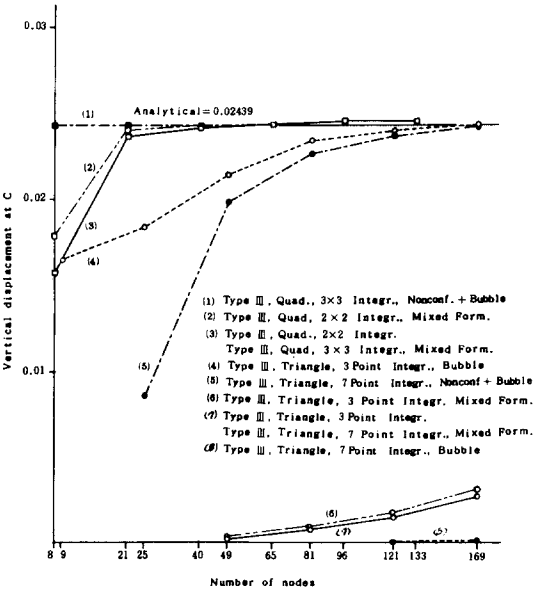

Fig.4. Effect of complementary measures. (pinched thin cylinder test case)

Ⅰ, Ⅱ and Ⅲ have been derived. The behavior of the type Ⅲ element has been closely examined through numerical tests. The element has properties similar to Armad's degenerate shell element, but shows better performance than the latter for standard benchmark problems. Reduce integration improves remarkably the performance of the type Ⅲ element of quadrilateral shape. But the element of triangular or disorted quadrilateral shape cannot take advantage of reduce integration and suffers from shear locking under thin shell situation. Combined application of reduced integration and a bubble mode is highly effective in relieving the locking phenomenon, but leads to failure for some cases due to spurious zero energy modes.A new method of controlling the spurious modes has been suggested in this study. The method does not use any artificial numbers such as e or α, and thus provides consistent control of spurious modes so that the generality of the element can be maintained.

9. REFERENCES.

1. Ahmad, S., B.M. Irons, and O.C. Zienkiewicz, Analysis of thick and thin shell structures be curved finite elements, *Int. J. Num. Meth. Engng.*, Vol.2., pp419-451, 1970.
2. Bazeley, G.P., Y.K. Cheung, B.M. Irons, and O.C. Zienkiewicz, Triangular elements in plate bending-conforming and non-conforming solution, *Proc. Conf. Matrix Meth. Struct. Mech.*, Wright-Patterson Air Force Base. Ohio, 1965.
3. Belytschko, T., C.S. Tsay, and W.K. Liu, A stabilization matrix for the bilinear mindlin plate element, *Comp. Meth. Appl. Mech. Engng.*, Vol.29, pp313-327. 1981.
4. Choi, C.K., Reduced integrated nonconforming plate element, *J. Engng. Mech.*, ASCE, Vol. 112, pp370-385, 1986.
5. Cook, R.D., More on reduce integration and isoparametric elements, *Int. J. Num. Meth. Engng.*, Vol.3, 1972.
6. Cook, R.D., *Concepts and Applications of Finite Element Analysis*, 2nd edn., John Wiley & Sons, New York, 1981.
7. Kavanagh, K.T., and S.W. Key, A note on selective and reduced integration techniques in the finite element method, *Int. J. Num. Meth. Engng.*, Vol., pp148-150, 1972.
8. Lee, J.Y., *A Finite Element for Shell Analysis and Its Application to Biological Objects*, Ph. D. Thesis, Cornell Univ., New York, 1986.
9. Lee, J. Y., *A Formulation of a Shell Finite Element Based on a New Method of Element Decomposition*, Research Report(Research No. 864-1301-002-1), Korea Science and Engineering Foundation, 1988.
10. Lee, S.W., and T.H.H. Pian, Improvement of plate and shell finite elements by mixed formulations, *AIAA J.*, Vol.1, pp29-34, 1978.
11. Stolarski, H., T.Belytschko, and N. Carpenter, A simple triangular curved shell element, *Engng. Comput.*, Vol.1, pp210-218, 1984.
12. Takemoto, H., and R.D. Cook, Some modifications of an isoparametric shell element, *Int. J. Num. Meth. Engng.*, Vol, pp401-405, 1973.
13. Tsach, U., Locking of thin plate / shell elements, *Int. J. Num. Meth. Engng.*, Vol.17, pp633-644, 1981.
14. Zienkiewicz, O.C., R.L. Taylor, and J.M. Too, Reduced integration technique in general analysis of plates and shells, *Int. J. Num. Meth. Eneng.* Vol.3, pp275-290, 1971.

(1988년 5월 30일 접수)